The Novel Vector-Fitting Approach for Time-Domain Modeling of the Propagation on Convex Obstacles in UWB Channels

P. Górniak[1]

Abstract– **In this paper we introduce the new approach for the derivation of a simple in form UTD impulse responses of a convex object in the form of 2D cylinder. We focus in the paper on the diffraction phenomenon. The impulse responses can be derived for impedance as well as dielectric object case. The impulse responses can be used for simulations of UWB EM wave propagation in channels containing convex obstacles of various physical properties, e.g. human body (modeled by dielectric cylinder). The impulse responses are derived by applying Vector Fitting approximation.**

1 INTRODUCTION

The purpose of the paper is to describe the procedure for the derivation of an UTD ray for a diffraction case on an impedance and a dielectric 2D cylinder. The procedure is an improved algorithm presented by authors in [1] for an ideal conductor case. Modeling of many convex obstacles in real world scenario with ideal conductor can be inaccurate, e.g. human body which effectively can be modeled by a dielectric object. It was shown by measurement results, e.g. [2] that for the case of such a dielectric object as human that shadows transmitting and receiving antennas positions, the dominant contribution to the EM field is given along a diffraction path (creeping ray). Therefore we extend the work from [1] to an impedance and a dielectric object case. The advantage of the impulse responses derived with the new approach is their simple form (sum of exponential functions) which can be calculated in time-domain very effectively. The impulse responses are obtained with the usage of Vector Fitting algorithm [3]. The vector fitting is made once for the considered range of values of convex object parameters. As a result we get closed form impulse responses whose poles and residues values are the same for all the considered values of convex object parameters.

The paper is organized as follows. In Section 2 we give the convex obstacle model in frequency-domain. Section 3 contains the procedure for the derivation of the impulse responses. In Section 4 the results of the verification of the new approach are presented. We make conclusions in Section 5.

2 Diffraction Ray Transfer Function

The parameters of the scenario of a diffraction ray creeping on a 2D cylinder placed in free space is shown in Fig. 1. Although the results presented in the article concern circular creeping ray path, they can be easily extended for application to an elliptical creeping ray path. The main parameters of the scenario in Fig. 1 are: θ – angular creeping distance, R – radius of an object. The cylinder has a permittivity and conductivity equal to ε_2 and σ respectively, while $\varepsilon_1 = \varepsilon_0$.
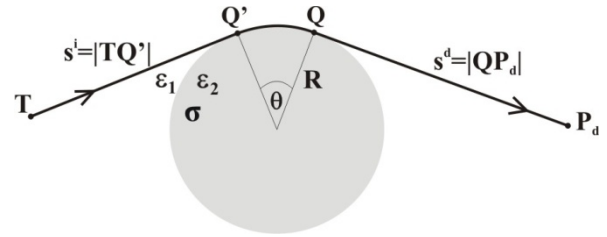

Figure 1: 2D model of a convex obstacle.

The UTD amplitude term of a transfer function of a creeping ray can be found in [4] (the delay and attenuation in the air factors are omitted).

$$H_A(\omega) = H_{A1}(\omega) + H_{A2}(\omega), \qquad (1)$$

where c is the speed of EM speed propagation in free space and:

$$H_{A1}(\omega) = \sqrt{\frac{c}{2\pi\omega \cdot \theta^2}} \cdot e^{-j\frac{\pi}{4}} F(X_d), \qquad (2)$$

$$H_{A2}(\omega) = -\left(\frac{2c \cdot R^2}{\omega}\right)^{1/6} e^{-j\frac{\pi}{4}} \begin{cases} p^*(\xi_d, q) \\ q^*(\xi_d, q) \end{cases} \qquad (3)$$

The transfer function of a ray contains two components (1). The first of them contains the transition function [4]. The second of them contains Fock scattering function which takes different forms depending on values of cylinder physical parameters [4]. Fock scattering functions can be expressed by the following integrals [5]:

$$\begin{cases} p^*(\xi_d, q) \\ q^*(\xi_d, q) \end{cases} = \frac{1}{\sqrt{\pi}} (C_1(\xi_d, q) + C_2(\xi_d, q)) \qquad (4)$$

where:

---

[1]Department of Electronics and Telecommunications, Poznan University of Technology, Poznan, Poland,
 e-mail: pgorniak@et.put.poznan.pl,

$$C_1(\xi_d, q_r) = \frac{e^{-j\frac{\pi}{6}}}{2} \times$$

$$\times \int_0^\infty \frac{\left[e^{-j\frac{\pi}{6}} Ai'(\tau) - q \cdot e^{j\frac{\pi}{6}} Ai(\tau)\right] e^{-j\cdot\xi_d \tau \cdot e^{-j\frac{2\pi}{3}}}}{e^{j\frac{\pi}{6}} Ai'\left(\tau \cdot e^{j\frac{2\pi}{3}}\right) - q \cdot e^{-j\frac{\pi}{6}} Ai\left(\tau \cdot e^{j\frac{2\pi}{3}}\right)} \times d\tau, \quad (5)$$

$$C_2(\xi_d, q) = -\frac{1}{2} \times$$

$$\times \int_0^\infty \frac{\left[Ai'(\tau) + q \cdot Ai(\tau)\right] e^{-j\cdot\xi_d \cdot \tau} d\tau}{e^{j\frac{\pi}{6}} Ai'\left(\tau \cdot e^{-j\frac{2\pi}{3}}\right) - q \cdot e^{-j\frac{\pi}{6}} Ai\left(\tau \cdot e^{-j\frac{2\pi}{3}}\right)}. \quad (6)$$

Variable q for an impedance and a dielectric cylinder case can be given by (7) and (8) respectively [6]:

$$q_C = -j \cdot \left(\frac{\omega \cdot R}{2c}\right)^{1/3} \left(\sqrt{\frac{j \cdot \sigma}{\omega \cdot \varepsilon_0}}\right)^m, \quad (7)$$

$$q_D = -j \cdot \left(\frac{\omega \cdot R}{2c}\right)^{1/3} \frac{\tilde{L}_C}{2R} \left(\sqrt{\varepsilon_r\left(1 + j\frac{\sigma}{\varepsilon_0 \varepsilon_r \omega}\right)}\right)^m, \quad (8)$$

where m is equal 1 and -1 for TM (soft) and TE (hard) polarization case and $\tilde{L}_C$ is given by [6]:

$$\tilde{L}_C = 2R \cdot \cos(\theta_C), \quad (8)$$

where θ_C is a refraction angle at cylinder-air boundary when incident angle is 90°.

3   The Derivation of an Impulse Response

The first component of the transfer function (1) can be rearranged into (9) [1].

$$H_{A1}(\omega) = \sqrt{\frac{L_d}{4\pi}} \cdot e^{-j\frac{\pi}{4}} \frac{F(X_{dsub})}{\sqrt{X_{dsub}}}. \quad (9)$$

where X_{dsub} is equal $\beta_0 L_d \theta^2/2$ and $L_d = s^i \cdot s^d/(s^i + s^d)$. After this rearrangement (8) is approximated using Vecor Fitting in X_{dsub} (normalized ω) domain. The limits of X_{dsub} are found by a calculation of its value for practical considered UWB scenarios. Finally (9) can be written in the form of (10) whose time-domain equivalent is (11), where C_{1j} and A_{1j} are residues and poles calculated with Vector Fitting.

$$H_{A1}(\omega) \approx \sqrt{\frac{L_d}{4\pi}} \cdot \sum_{j=1}^{J} \frac{C_{1j} \cdot 2c/L_d\theta^2}{j\omega + A_{1j} \cdot 2c/L_d\theta^2}. \quad (10)$$

$$h_{A1}(t) \approx \sqrt{\frac{L_d}{4\pi}} \cdot \sum_{j=1}^{J} \frac{C_{1j} 2v}{L\theta^2} e^{-\frac{A_{1j} \cdot 2v}{L\theta^2}t} \quad (11)$$

In order to find a time-domain equivalent of (3) it is rearranged to the following form:

$$H_{A2}(\omega) = \sqrt{R\theta} e^{-j\frac{\pi}{4}} \frac{\begin{cases} p^*\left(\xi_{dsub}^{1/3}, q\right) \\ q^*\left(\xi_{dsub}^{1/3}, q\right) \end{cases}}{\sqrt{\xi_{dsub}^{1/3}}} \quad (12)$$

where $\xi_{dsub} = \theta^3 \omega \cdot R \cdot (2c)^{-1}$ and q for an impedance and a dielectric cylinder case can be expressed for TM polarization by (13) and (14) respectively.

$$q_C = e^{-j\pi/4}\left(\xi_{dsub}\right)^{-1.6}\sqrt{u_{Csub}} \quad (13)$$

$$q_D = -j \cdot \left(\frac{\xi_{dsub}}{u_{D3sub}}\right)^{1/3} \frac{\tilde{L}_C}{2R}\left(\sqrt{u_{D2sub} + j\frac{u_{D1sub} \cdot u_{D3sub}}{\xi_{dsub}}}\right) \quad (14)$$

where $u_{Csub} = 60\pi \cdot R \cdot \sigma \cdot \theta$, $u_{D1sub} = 60\pi \cdot R \cdot \sigma$, $u_{D2sub} = \varepsilon_r$, $u_{D3sub} = \theta^3$.

Quantity (8) in (14) is also the function of ξ_{dsub}, u_{D1sub}, u_{D2sub} and u_{D3sub}. The Vector Fitting approximation of (12) is performed in ξ_{dsub} (normalized ω) domain for given tabulated (sampled) values of u_{Csub} or set of values u_{D1sub}, u_{D2sub} and u_{D3sub}. The limits of u_{Csub}, u_{D1sub}, u_{D2sub} and u_{D3sub} values are calculated according to limits of values of considered cylinder parameters and band limits of considered UWB signals.

For an impedance cylinder case real and imaginary parts of (12) are continuous functions with respect to u_{Csub} for ξ_{dsub}=constant. Therefore each consecutive Vector Fitting Approximation   (for consecutive sampled u_{Csub} values) may be done by implementing the adjustment of the previously found poles and residues values (for previous u_{Csub} value). In a consequence each of poles and residues is a continuous function of u_{Csub}.

In order to perform analogous manipulations for the case of a dielectric cylinder u_{D1sub}, u_{D2sub} and u_{D3sub} variables have to be formed into the one variable in the way that the real part and imaginary part of (12) are continuous functions of this one variable for ξ_{dsub}=constant. Such a variable can be expressed in the form $u_{Dsub} = u_{D1sub} \cdot u_{D3sub}/u_{D2sub}$.

In the end the approximated form of (12) for an impedance and a dielectric cylinder case is given by (15) and (16) respectively and the corresponding time-domain functions are given by (17) and (18):

$$H_{A2C}(\omega) \approx \sqrt{R\theta} \cdot \sum_{k=1}^{K} \frac{C_{2Ck}(\sigma, R, \theta) \cdot 2c/R\theta^3}{j\omega + A_{2Ck}(\sigma, R, \theta) \cdot 2c/R\theta^3}, \quad (15)$$

$$H_{A2D}(\omega) \approx \sqrt{R\theta} \cdot \sum_{k=1}^{K} \frac{C_{2Dk}(\varepsilon_r, \sigma, R, \theta) \cdot 2c/R\theta^3}{j\omega + A_{2Dk}(\varepsilon_r, \sigma, R, \theta) \cdot 2c/R\theta^3}, \quad (16)$$

$$h_{A2C}(t) \approx \sqrt{R\theta} \times$$
$$\times \sum_{k=1}^{K} \frac{C_{2Ck}(\sigma,R,\theta)}{R\theta^3 (2c)^{-1}} exp\left(-\frac{A_{2Ck}(\sigma,R,\theta) \cdot 2c}{R\theta^3}\right), \quad (17)$$

$$h_{A2D}(t) \approx \sqrt{R\theta} \times$$
$$\times \sum_{k=1}^{K} \frac{C_{2Dk}(\varepsilon_r,\sigma,R,\theta)}{R\theta^3 (2c)^{-1}} exp\left(-\frac{A_{2Dk}(\varepsilon_r,\sigma,R,\theta) \cdot 2c}{R\theta^3}\right), \quad (18)$$

where $C_{2Ck}(\sigma,R,\theta)$, $A_{2Ck}(\sigma,R,\theta)$ and $C_{2Dk}(\sigma,R,\theta)$ and $A_{2Dk}(\sigma,R,\theta)$ are the functions of residues and poles for an impedance and a dielectric cylinder case respectively.

4   Numerical Calculations Examples

In this section we present the results of simulations of diffraction of exemplary UWB pulse on an impedance and a dielectric 2D cylinder. We compare IFFT results incorporating (1) with the results obtained directly in the time-domain by applying the impulse response, derived with the procedure described in the previous section. We consider the following range of values for the scenario of a diffraction on a cylinder: $R\in<0.2m, 0.3m>$, $\theta\in<10^{-4}rad, 10^{-1}rad>$, $f\in<0.5GHz, 10GHz>$. Then the values of normalized pulsation ξ_{dsub} are in the range $<10^{-10}, 10^{0}>$. Analogous considerations are made for X_{dsub} letting a value of L_d be in a range $<0.5, 4.0>$. Then number of poles and residues in (11) and (17), (18) equals to 10 and 20 respectively when the maximum allowed relative deviation of approximation is 0.5%. The range of a conductivity value for an impedance cylinder case is set to $<10^3, 10^6>$s/m. The ranges of physical parameters values of a dielectric cylinder are set to: $\sigma\in<1, 10>$s/m, $\varepsilon_r\in<35, 55>$. We derived functions of poles and residues for an impedance and dielectric a cylinder case by treating u_{Csub} and u_{Dsub} as time variables respectively and applying FFT and Vector Fitting approximation. The exemplary results for impedance and dielectric cylinder case are shown in Fig 2. and Fig. 3 respectively. The incident UWB pulse is given by the following formula:

$$p(t) = \left[1 - 4\pi\left(\frac{t-t_c}{a}\right)^2\right]exp\left(-2\pi\left(\frac{t-t_c}{a}\right)\right) \quad (19)$$

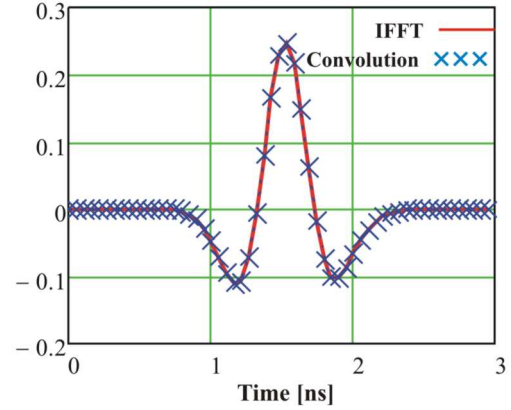The t_c and a values are set to 1.5 ns and 0.7 ns respectively.

Figure 2: Distorted UWB Gauss pulse for parameters values: R = 0.25m, θ = 0.1, σ=10^3, L_d=1.0.

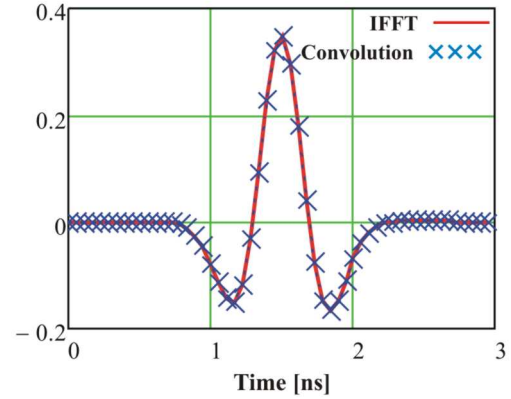Figure 3: Distorted UWB Gauss pulse for parameters values: R = 0.25m, θ = 0.01, σ=5, ε_r=50, L_d=1.0.

4   Conclusions

The aim of the article was to present the new approach for derivation of an impulse response of an aimpedance and a dielectric convex object. This object can be an effective model of a real convex obstacles, e.g. human body, that can occur in an UWB channel.

We verified the new method by performing the simulations with the usage of the impulse response derived for the cinsidered limits of scenario parameters values. We showed that there is a very good agreement between convolution and IFFT (reference) results (Fig. 2 and Fig. 3).

The form of the impulse responses are very simple, and can be effectively applied to simulations of UWB wave propagation on convex obstacles. We can apply direct analytical calculations of convolutions or use faster recursive numerical procedures of convolutions and take advantage of the fact that the components of the impulse responses describe low-pass filters. Then part of the impulse response components can be omitted during calculation of a particular ray response or can be approximated by a delayed delta Dirac function

References

[1] P. Górniak, W. Bandurski, "The New Vector Fitting Approach to Modeling of UWB Channels Containing Convex Obstacles", 6th European Conference on Antennas and Propagation, Prague, 26-30 March 2012.

[2] Ch. Kim; Dong-Woo Ha; S. Sangodoyin, "UWB propagation measurements in BAN scenarios", International Symposium on Communication Systems, Networks & Digital Signal Processing (CSNDSP), 18-20 July 2012, pp.1-6

[3] B. Gustavsen, "Rational approximation of frequency domain response by vector fitting", IEEE Tran. on Power Delivery, vol.14, no. 3, 1999, pp. 1052-1061.

[4] T. Ida, T. Ishihara, K. Goto, "Frequency-Domain and Time-Domain Novel Uniform Asymptotic Solutions for Scattered Fileds by an Impedance Cylinder and a Dielectric Cylinder", IEICE Transactions on Electronics, vol. E88-C, no. 11, pp. 2124–2135, November 2005

[5] L. Pearson, "A scheme for Automatic Computation of Fock-Type Integrals", IEEE Transactions on Antennas and Propagation, vol. 35, no. 10, pp. 1111–1118, October 1987

[6] T. Sasamori, T.Uno, S. Adachi, "High-Frequency Analysis of Electromagnetic Scattering due to a Dielectric Cylinder" ", IEICE Transactions on Electronics, vol. J78-C-I, no. 1, pp. 9–19, January 1995